doi:10.1017/S1431927620013124
Microsc. Microanal. 26 (Suppl 2), 2020

Direct Mapping of Electrostatic Potentials by Momentum-resolved STEM and Electron Holography - A Conceptual Comparison

Knut Müller-Caspary, Florian Winkler, Hoel Laurent Robert, Achim Strauch and Juri Barthel

Forschungszentrum Jülich, Jülich, Nordrhein-Westfalen, Germany

The simultaneous access to both subatomic real space details by aberration correction, and precise momentum space features via ultrafast diffraction cameras [1-4] employed in STEM has enhanced the versatility of this imaging mode drastically. Because full diffraction patterns are available for each scan position, formerly static annular bright- and dark field imaging can now be replaced by an angular multi-range analysis performed using software after the acquisition, e.g., to measure several properties of the specimen independently and simultaneously [5]. Most importantly, this 4-dimensional momentum-resolved STEM data is nowadays routinely employed for electron ptychography [6] or first moment imaging [7] (FM). Under certain conditions such as the validity of the phase object approximation, these STEM methods are capable of providing either the phase of an object transmission function or its gradient, respectively, and hence in principle allow for the direct measurement of electrostatic potentials and electric fields. This rapid methodological development in the field of STEM during the last decade suggests a conceptual comparison to TEM-based counterparts for phase and potential retrieval, namely off-axis electron holography (EH), including a discussion of electron-optical and specimen parameters affecting accuracy and precision [8].

In this contribution, we start by analysing conceptual differences between FM-STEM and off-axis electron holography which can be subdivided into three main topics. First, it is checked to which extent the interaction of electrons with the specimen must be simplified so as to establish a direct relation between FM and atomic-scale electric fields, as well as between reconstructed phases in EH and Coulomb potentials. By general, formal considerations, FM-STEM is acting within the limits of the phase approximation to yield the projected electric field of the specimen convolved with the squared inverse Fourier-transformed probe-forming aperture. In contrast, EH relies on the weak phase approximation to directly yield the projected Coulomb potential, convolved with the inverse Fourier transform of the objective aperture. Therefore, both methods deliver different quantities even if all approximations inherent to the respective direct interpretability are justified.

Second, we focus on the impacts of dynamical scattering on FM-STEM and EH. The very different convergent and parallel illumination settings cause the direct interpretability to break down at very different thicknesses, which we found by extensive multislice simulations. It turnes out that interpreting the reconstructed phase in terms of the (weak) phase approximation in EH leads to a root-mean-square error which increases approximately linearly with specimen thickness. In that respect, FM-STEM is found more robust on the one hand as it retains small errors below those of EH over a broader range of thicknesses. On the other hand, the accuracy of FM-STEM based potential measurements is strongly dependent on imaging at an optimum focus. For example, FM-STEM can become much more inaccurate than EH already at 3nm specimen thickness in $SrTiO_3$, or remain twice as accurate as EH up to more than 6nm, depending on focus.

Third, the dependence the focus for maximum contrast of several STEM signals is studied as a function of specimen thickness in simulation and experiment. Here, we find that FM and Z-contrast foci can differ significantly at elevated specimen thicknesses. Whereas this has minor impact on the direct mapping of atomic-scale electrostatic fields which is limited to thin specimen consisting of a few atomic layers, care must be taken in FM-STEM experiments aiming at, e.g., the mapping of spontaneous, piezo- and ferroelectric polarisations in which specimen thicknesses of several tens of nanometers are preferred [9].

In the second part, we broaden the view on momentum-resolved STEM methodology by including electron ptychography reconstructions using different established algorithms. In addition to the aforementioned effects of dynamical scattering, we consider the dose-efficiency of both FM-STEM and ptychography to discuss possible routes for high-contrast imaging in the field of soft matter. In that respect, first examples will be demonstrated that compare the contrast of different momentum-resolved STEM approaches achieved in specimen taken from structural biology applications.

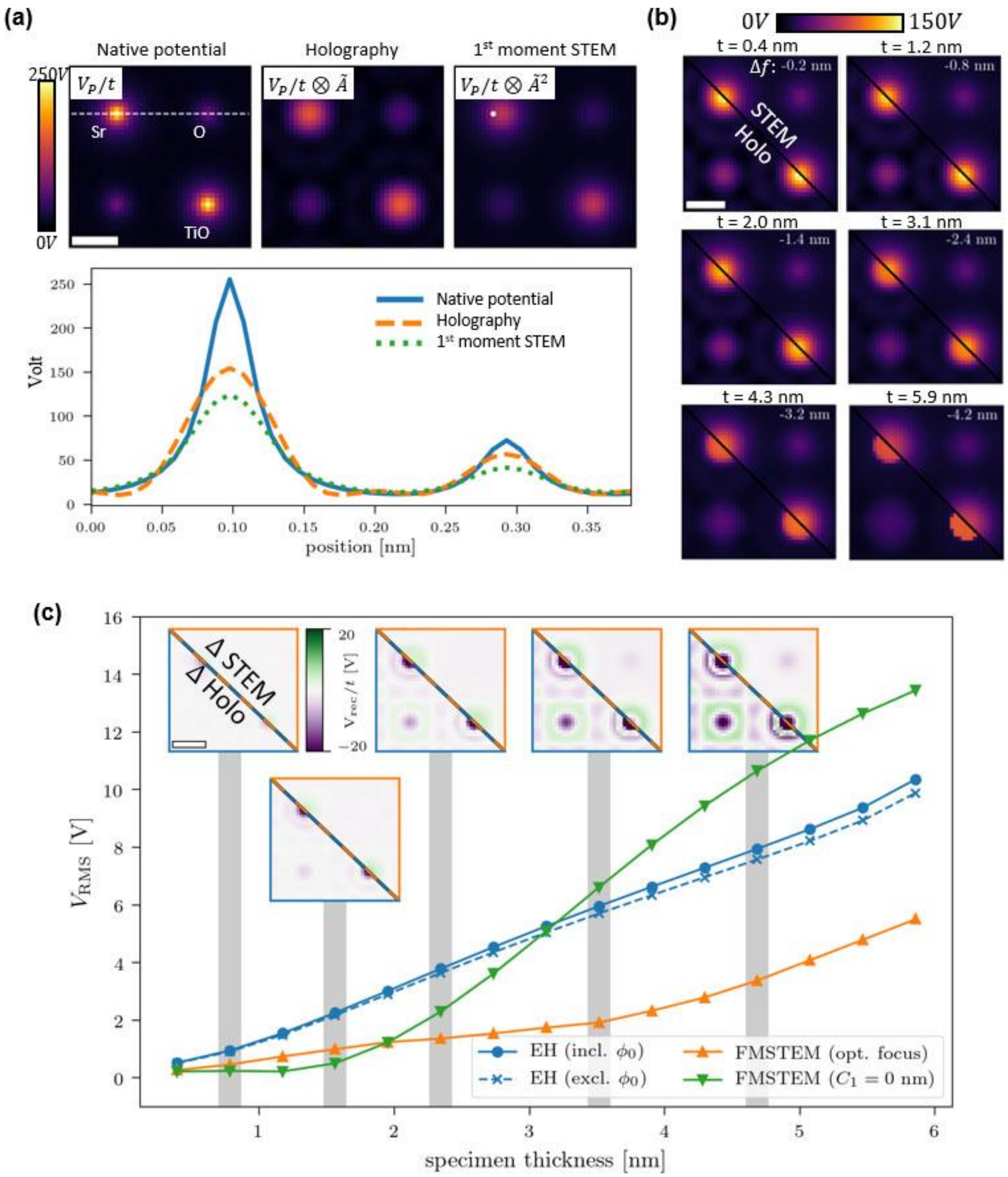

https://doi.org/10.1017/S1431927620013124 Published online by Cambridge University Press

Figure 1. Fig. 1: Comparison of first moment STEM with electron holography. (a) True projected potential of Strontium Titanate and the result of an ideal measurement employing EH and FM-STEM using the same aperture. In EH, the convolution kernel consists of the inverse Fourier transfor of the aperture, whereas it is its square in FM-STEM. (b) Simulated measurement of the Coulomb potential for EH and FM-STEM (integrated electric field) as a function of specimen thickness. In EH, plateaus evolve at atomic columns with increasing thickness. In FM-STEM, imaging at optimum defocus (top right) is necessary for reliable interpretation of measured potential maps. (c) Thickness-dependent root-mean-square error associated with the neglect of dynamical scattering when interpreting reconstructed phase (EH) or FM maps (STEM). The error increases linearly for EH and is larger than for FM-STEM if the correct focus is chosen.

References

[1] Müller, K.; Ryll, H.; Ordavo, I.; Ihle, S.; Strüder, L.; Volz, K.; Zweck, J.; Soltau, H.; Rosenauer, A., Appl. Phys. Lett., 2012, 101, 212110.
[2] Plackett, R.; Horswell, I.; Gimenez, E. N.; Marchal, J.; Omar, D.; Tartoni, N., J. Instrum., 2013, 8, C01038.
[3] Müller-Caspary, K.; Oelsner, A.; Potapov, P., Appl. Phys. Lett., 2015, 107, 072110.
[4] Tate, M. W.; Purohit, P.; Chamberlain, D.; Nguyen, K. X.; Hovden, R.; Chang, C. S.; Deb, P.; Turgut, E.; Heron, J. T.; Schlom, D. G.; Ralph, D. C.; Fuchs, G. D.; Shanks, K. S.; Philipp, H. T.; Muller, D. A.; Gruner, S. M., 2016, 22, 237-249.
[5] Müller-Caspary, K.; Oppermann, O.; Grieb, T.; Krause, F. F.; Rosenauer, A.; Schowalter, M.; Mehrtens, T.; Beyer, A.; Volz, K.; Potapov, P., Scientific Reports, 2016, 6, 37146.
[6] Rodenburg, J. M.; McCallum, B. C.; Nellist, P. D., Ultramicroscopy, 1993, 48, 304-314.
[7] Müller, K.; Krause, F. F.; Béché, A.; Schowalter, M.; Galioit, V.; Löffler, S.; Verbeeck, J.; Zweck, J.; Schattschneider, P.; Rosenauer, A.: Nature Comm., 2014, 5, 5653.
[8] Winkler, F.; Barthel, J.; Dunin-Borkowski, R. E.; Müller-Caspary, K., Ultramicroscopy, 2020, 210, 112926.
[9] Müller-Caspary, K.; Grieb, T.; Müßener, J.; Gauquelin, N.; Hille, P.; Schörmann, J.; Verbeeck, J.; Aert, S. V.; Eickhoff, M.; Rosenauer, A., Phys. Rev. Lett., 2019, 122, 106102.